

- 1 Okamoto, K., and Aoki, K., Jap. Circ. J. 27 (1963) 282.
- 2 Takeichi, N., and Boone, Ch. W., Cell. Immun. 27 (1976) 52.
- 3 Takeichi, N., Suzuki, K., Okayasu, T., and Kobayashi, H., Clin. exp. Immun. 40 (1980) 120.
- 4 Takeichi, N., Ba, D., and Kobayashi, H., Cell. Immun. 60 (1981) 181.
- 5 Takeichi, N., Suzuki, K., and Kobayashi, H., Eur. J. Immun. 11 (1981) 483.
- 6 Ba, D., Takeichi, N., Kodama, T., and Kobayashi, H., J. Immun. 128 (1982) 1211.
- 7 Strausser, H. R., Thymus 5 (1983) 19.
- 8 Bendich, A., Belisle, E. H., and Strausser, H. R., Biochem. biophys. Res. Commun. 99 (1981) 600.
- 9 Norman, R. A., Dzielak, D. J., Bost, K. L., Cuchens, M. A., and Khraibi, A. A., Physiologist 26 (1983) A-48 (Abstr. 26.9).
- 10 Norman, R. A., Dzielak, D. J., Bost, K. L., Khraibi, A. A., and Gal- loway, P. G., J. Hypertension 3 (1985) 261.
- 11 Khraibi, A. A., Norman, R. A., and Dzielak, D. J., Physiologist 25 (1982) 337 (Abstr. 70.7).
- 12 Khraibi, A. A., Norman, R. A., and Dzielak, D. J., Am. J. Physiol. 247 (1984) H722.
- 13 Borel, J. F., Rüegger, A., and Stähelin, H., Experientia 32 (1976) 777.
- 14 Britton, S., and Palacios, R., Immun. Rev. 65 (1982) 5.
- 15 Wagner, H., Trans. Proc. 15 (1983) 523.
- 16 Leenen, F. H., and Jong, W. de, J. appl. Physiol. 31 (1971) 142.
- 17 Borel, J. F., Feurer, C., Grubler, H. V., and Stähelin, H., Agent Action 6 (1976) 468.
- 18 Borel, J. F., Feurer, C., and Magnée, C., Immunology 32 (1977) 1017.
- 19 Okuda, T., and Grollman, A., Tex. Rep. Biol. Med. 25 (1967) 257.
- 20 Provoost, A. P., and Keyzer, M. H. de, in: Handbook of Hyper- tension, vol. 4: Experimental and genetic models of hypertension, p. 518. Ed. W. de Jong. Elsevier Science Publishers, Amsterdam 1985.
- 21 Kristensen, B. Ø., J. Hypertension 2 (1978) 571.
- 22 Gualde, N., Michel, J. P., and Safar, M. E., Lancet 2 (1978) 897.
- 23 Löw, B., Schersten, B., Sanetor, G., Thulin, T., and Mitelman, F., Lancet 2 (1975) 695.

0014-4754/87/040403-03\$1.50 + 0.20/0

© Birkhäuser Verlag Basel, 1987

## Differential sensitivity of amphibian nodal and paranodal K<sup>+</sup> channels to 4-aminopyridine and TEA

C. L. Schauf

Department of Biology, Indiana University – Purdue University, School of Science at Indianapolis, 1125 East 38th Street, Indianapolis (Indiana 46223, USA), 31 July 1986

**Summary.** Voltage-dependent K<sup>+</sup> channels are blocked by several drugs, including 4-aminopyridine (4-AP) and tetraethylammonium (TEA). 4-AP is most widely used to localize K<sup>+</sup> channels in mammalian and non-mammalian nerve fibers, but 4-AP and TEA alter various K<sup>+</sup> channels and/or preparations in specific ways. The reason is not known, in part because dissociation constants for 4-AP and TEA have not been measured for nodal and internodal K<sup>+</sup> channels in the same fibers. Smith and Schauf<sup>1</sup> showed that the density of nodal versus paranodal K<sup>+</sup> channels in frog nerves depends on fiber diameter. This size dependence was used to determine the relative sensitivity of nodal and internodal K<sup>+</sup> channels to 4-AP and TEA, and to compare voltage- and time-dependent activation. The results show nodal and internodal K<sup>+</sup> channels activate similarly. However, internodal channels are selectively blocked by 4-AP while TEA is more effective on nodal channels. A high sensitivity of internodal K<sup>+</sup> channels may explain why 4-AP improves symptoms in diseases such as multiple sclerosis.

**Key words.** Potassium channels; 4-aminopyridine; tetraethylammonium; *Rana pipiens* nerves; voltage clamp; lyssolecithin; nodal channels; internodal channels.

The drug 4-aminopyridine (4-AP) blocks the classical delayed rectifier K<sup>+</sup> channel in nonmyelinated axons and amphibian nodes of Ranvier and has been used to determine their distribution<sup>2-7</sup>. In mammalian myelinated nerve K<sup>+</sup> channels are excluded from nodes<sup>8-10</sup>. Exposure of a mammalian internode in demyelination results in the appearance of outward K<sup>+</sup> currents and 4-AP sensitivity<sup>11-17</sup>. 4-AP prolongs action potentials in immature and regenerating mammalian nerve<sup>12-14,16,18-20</sup>. However, sensitivity to 4-AP does not localize K<sup>+</sup> channels to nodes; it indicates electrical and chemical accessibility. Immature and regenerating fibers may lack nodal K<sup>+</sup> channels and differ from mature nerve in the access of internodal channels to 4-AP. Potassium channels are also blocked by tetraethylammonium (TEA) and the relative effect of 4-AP and TEA varies. For example, TEA does not affect many 4-AP sensitive mammalian nonmyelinated or myelinated axons<sup>20,21</sup> and is relatively ineffective on internodal K<sup>+</sup> channels<sup>12,13,22,23</sup>.

In animal models 4-AP restores conduction in demyelinated blocked fibers<sup>12,15,24</sup> and symptoms in multiple sclerosis (MS) are improved by 5–20 mg 4-AP<sup>25,26</sup>. Invertebrate axons and frog fibers have dissociation constants of 0.5 mM<sup>5</sup> and 10 μM<sup>6,27</sup>, and 1-mM 4-AP is usually used to detect K<sup>+</sup> channels<sup>16,17,19,20,26,28</sup>. In MS patients plasma 4-AP levels were about 1 μM. The small amount of 4-AP needed could result from a higher sensitivity of internodal K<sup>+</sup> channels to 4-AP. Since K<sup>+</sup> currents and 4-AP access both vary, comparison of 4-AP sensitivity requires a system where nodal and internodal K<sup>+</sup> channels can be voltage-clamped, so a fiber serves as its own control. Nodal K<sup>+</sup> conduc-

tance in 16–18-μm frog fibers is 20–30% of the Na<sup>+</sup> conductance and is increased by lyssolecithin (LPC). In 8–10-μm fibers there is no K<sup>+</sup> current unless LPC is used<sup>1</sup>. This diameter-dependence was used to compare K<sup>+</sup> channels. LPC-dependent channels were more sensitive to 4-AP than LPC-independent nodal channels, while TEA acts primarily on nodal channels. The size-dependent segregation of K<sup>+</sup> channels in frog fibers also allows a comparison of K<sup>+</sup> activation. While similar, there is a slight increase in the relative number of paranodal channels activated at low voltages compared to nodal channels.

**Methods.** Single 8–10-μm or 16–18-μm fibers of *Rana pipiens* were voltage-clamped in 115 mM NaCl, 2.5 mM KCl, 1.8 mM CaCl<sub>2</sub>, and 5 mM Tris<sup>1,29,30</sup>. Fiber ends were in isotonic KCl; pH was 7.30; and the temperature was 18–20°C. Fibers were classed as sensory or motor based on the initial rate of decline of the action potential<sup>31</sup>. Fibers were held at –80 mV<sup>32</sup>. A 50-ms hyperpolarization was followed by 10-ms depolarizations to voltages between –40 mV and +100 mV. Leakage and capacity currents were determined for each fiber and subtracted during ionic current measurements. Currents were converted to conductances using experimentally determined values for the Na<sup>+</sup> equilibrium potential and a calculated value of –97 mV for the K<sup>+</sup> equilibrium potential<sup>1,30,32</sup>. Nodal and internodal resistances were measured<sup>33</sup> because nodal capacitance determines exposed membrane area and internodal resistance gives current. The Na<sup>+</sup> equilibrium potential was monitored because internal Na<sup>+</sup> blocks K<sup>+</sup> channels, leading to an apparent lack of K<sup>+</sup> conductance<sup>34</sup>. Data was used only if there was no change.

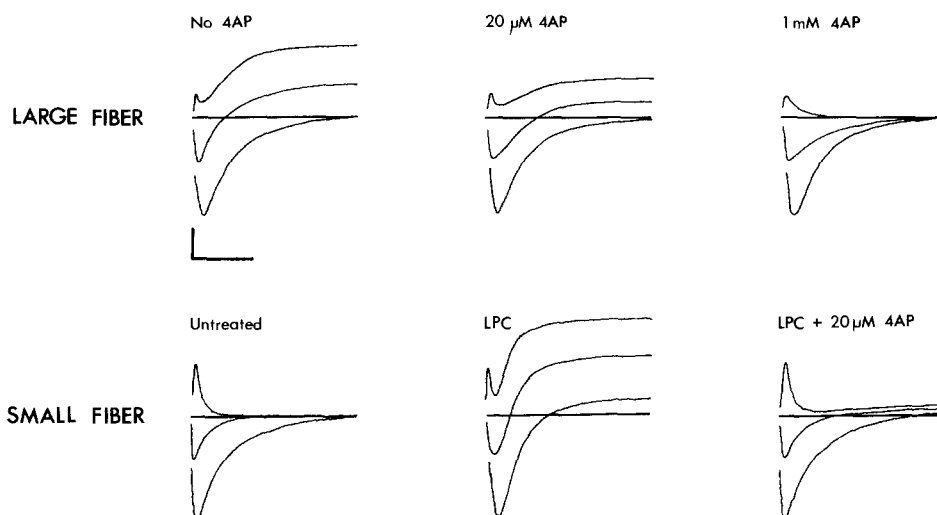


Figure 1. Currents for depolarizations to  $-30$  mV,  $+20$  mV, and  $+70$  mV in normal and lysolecithin-treated frog myelinated nerve fibers and the effect of 4-AP. The records in the upper portion of the figure show the currents in a  $17\text{-}\mu\text{m}$  fiber, while those in the lower portion were recorded from a  $9\text{-}\mu\text{m}$  fiber. In the first case there is normally a significant outward  $\text{K}^+$  current (left-hand records) that is blocked by 4-AP (center and right-hand records) without any effect on nodal  $\text{Na}^+$  currents. Normal, freshly dissected  $8\text{--}10\text{-}\mu\text{m}$  fibers lack  $\text{K}^+$  currents (records in the lower left-hand part of the figure), but  $\text{K}^+$  currents appear after exposure to  $1\text{ mg/ml}$  lysolecithin (lower, center records labeled LPC). LPC-induced currents are completely blocked by  $20\text{ }\mu\text{M}$  4-AP (records at the lower right), a concentration that only blocks  $50\%$  of the  $\text{K}^+$  current in  $16\text{--}18\text{-}\mu\text{m}$  fibers. The current calibration is  $16\text{ nA}$  for the  $17\text{-}\mu\text{m}$  fiber and  $8\text{ nA}$  for the  $9\text{-}\mu\text{m}$  fiber, while the time scale is  $2\text{ ms}$  for both. The  $\text{K}^+$  conductance for the  $9\text{-}\mu\text{m}$  fiber was  $0.05 \times 10^{-7}\text{ S}$  before LPC and increased to  $0.20 \times 10^{-7}\text{ S}$  following the application of LPC. The  $\text{K}^+$  conductance of the  $17\text{-}\mu\text{m}$  fiber was  $1.50 \times 10^{-7}\text{ S}$  prior to the application of 4-AP. The  $\text{Na}^+$  conductance of the  $9\text{-}\mu\text{m}$  fiber was  $0.89 \times 10^{-7}\text{ S}$ , while that for the  $9\text{-}\mu\text{m}$  fiber was  $4.95 \times 10^{-7}\text{ S}$ .

The size-dependence of the  $\text{K}^+$  conductance is not always apparent<sup>35</sup>. The reason is unknown since all studies have paid careful attention to  $\text{Na}^+$  accumulation and other possible artifacts<sup>1,35</sup>. To avoid this problem, nodal and paranodal  $\text{K}^+$  currents were defined operationally with nodal currents referring to those seen in untreated fibers and paranodal currents those following paranodal disruption induced by adding  $1\%$  lysolecithin to the  $50\text{--}100\text{ }\mu\text{m}$  recording pool. In untreated fibers the capacity transient was one exponential ( $40\text{--}60\text{-}\mu\text{s}$  time constant), nodal capacity was  $1.4\text{--}1.6\text{ pF}$ , and nodal resistance  $34\text{--}46\text{ megohms}$ . After LPC the capacity current has fast ( $40\text{--}60\text{-}\mu\text{s}$  time constant) and slow ( $1\text{ ms}$ ) components. The integral of the fast component was the same as untreated fibers, but the integral of the slow component varied with the paranodal area exposed. LPC elevated nodal capacitance (up to  $55\text{ pF}$ ) and all of the increase occurred in the slow component. Since nodal capacitance often increased without a visible change, LPC may disrupt the axoglial junction but not cause demyelination.

**Results.** Experiments were performed on untreated fibers lacking outward current where large  $\text{K}^+$  conductances can be induced by LPC; and on LPC-insensitive fibers. Figure 1 shows that 4-AP selectivity blocks LPC-dependent, presumably paranodal  $\text{K}^+$  channels. The left-hand records are from untreated  $16\text{--}18\text{-}\mu\text{m}$  (top) and  $8\text{--}10\text{-}\mu\text{m}$  (bottom) fibers with  $\text{Na}^+$  equilibrium potentials of  $+52\text{ mV}$  and  $+54\text{ mV}$  respectively. In  $16\text{--}18\text{-}\mu\text{m}$  fibers external  $20\text{-}\mu\text{M}$  4-AP decreased the outward  $\text{K}^+$  currents by  $45\text{--}50\%$  at all voltages, but had no effect on the magnitude and time course of the  $\text{Na}^+$  currents (top center records) or on nodal capacity and internodal resistance. At  $1\text{ mM}$ , 4-AP completely eliminated outward  $\text{K}^+$  currents, again without altering the  $\text{Na}^+$  current (upper right records). The filled circles in figure 2 show the dose-response curve for 4-AP obtained in two different  $16\text{--}18\text{-}\mu\text{m}$  fibers. The solid line, calculated assuming a single binding site and an effective dissociation constant of  $20\text{ }\mu\text{M}$ , provides a good fit to the experimental data over the entire range of concentrations tested.

LPC causes a large increase in the outward current in  $8\text{--}10\text{-}\mu\text{m}$  fibers, but there was no change in  $\text{Na}^+$  currents and the  $\text{Na}^+$  equilibrium potential remained at  $+54\text{ mV}$  (bottom center records). LPC-induced outward currents were accompanied by a

$14\text{-fold}$  increase in nodal capacitance measured by integrating the total (fast and slow components) uncompensated capacity current. In LPC-treated fibers,  $20\text{-}\mu\text{M}$  4-AP completely eliminated the outward current (bottom right records in fig. 1). The dose-response curve for 4-AP for two different fibers, shown by the open circles in figure 2, is consistent with a decrease in the apparent dissociation constant from  $20\text{ }\mu\text{M}$  to  $4\text{--}5\text{ }\mu\text{M}$ . That is, paranodal  $\text{K}^+$  channels exposed by LPC are more sensitive to 4-AP than are LPC-independent nodal  $\text{K}^+$  channels.

While 4-AP sensitivity of  $\text{K}^+$  currents in untreated  $16\text{--}18\text{-}\mu\text{m}$  fibers and LPC-treated  $8\text{--}10\text{-}\mu\text{m}$  fibers differs,  $\text{K}^+$  activation is nearly identical. Figure 3 shows the time constants for  $\text{K}^+$  activation in both cases ( $T_n$  with  $n = 2$ , see Bergman<sup>34</sup>). For voltages above  $-50\text{ mV}$  steady-state conductance-voltage curves also superimposed. Below  $-50\text{ mV}$  there appeared to be a slightly larger  $\text{K}^+$  conductance in LPC-treated  $8\text{--}10\text{-}\mu\text{m}$  fibers, but uncertainties in estimating the leakage current make this result less secure. A difference in the 'foot' of the activation curve would support the contention that paranodal  $\text{K}^+$  channels contribute to the resting potential<sup>18</sup>. In a few experiments the internodes in the lateral pools of the chamber were cut as short as possible to let  $\text{K}^+$  enter the periaxonal space. After  $15\text{--}20\text{ min}$ , the node in the recording pool depolarized by  $14\text{--}17\text{ mV}$ .

While paranodal  $\text{K}^+$  channels are more readily blocked by 4-AP, they are less sensitive to TEA. Figure 4 shows the dose-response curve for TEA in two different untreated  $16\text{--}18\text{-}\mu\text{m}$  fibers (filled circles) and two  $8\text{--}10\text{-}\mu\text{m}$  LPC-treated fibers (open circles). The dissociation constant for TEA on LPC-induced  $\text{K}^+$  currents was  $5\text{ mM}$ , ten times higher than for nodal  $\text{K}^+$  channels ( $0.5\text{ mM}$  — shown as the solid line in fig. 4).

The effects of 4-AP and TEA on  $12\text{-}\mu\text{m}$  fibers with small but measureable  $\text{K}^+$  currents were examined in a few cases. Untreated fibers had resting conductances of  $0.10\text{--}0.15 \times 10^{-7}\text{ S}$ . The dissociation constants for 4-AP and TEA were  $20\text{ }\mu\text{M}$  and  $0.5\text{ mM}$  respectively in untreated  $12\text{-}\mu\text{m}$  fibers, results identical to those in  $16\text{--}18\text{-}\mu\text{m}$  fibers. After LPC treatment the  $\text{K}^+$  conductance ranged from  $0.22\text{--}0.31 \times 10^{-7}\text{ S}$  in  $12\text{-}\mu\text{m}$  fibers. Dose-response curves for 4-AP and TEA on LPC-induced  $\text{K}^+$  currents in  $12\text{-}\mu\text{m}$  fibers were compared with those in LPC-treated  $8\text{--}10\text{-}\mu\text{m}$  frog fibers. The dissociation constant for 4-AP on the incre-

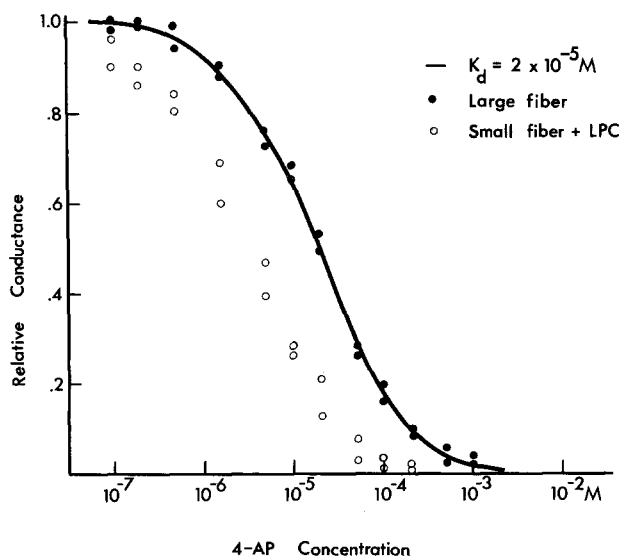


Figure 2. Dose-response curves for 4-AP in two different 16–18- $\mu$ m (filled circles) and 8–10- $\mu$ m (open circles) fibers. The ordinate shows the  $K^+$  conductance in the presence of 4-AP relative to that prior to drug application (the effects of 4-AP were reversible and values of the  $K^+$  conductance before and after 4-AP differed by less than 10%). The solid line is expected for a single site having an effective binding constant of  $2 \times 10^{-5}$  M and accurately describes the response of 16–18- $\mu$ m fibers. The behavior of 8–10- $\mu$ m fibers is consistent with a shift of this dissociation curve to the left along the abscissa so that the effective binding constant is reduced to  $5 \times 10^{-6}$  M.

mental  $K^+$  current in 12- $\mu$ m fibers was 4  $\mu$ M, while that for TEA was 3–5 mM. Paranodal  $K^+$  channels in 12- $\mu$ m fibers thus resemble those in 8–10- $\mu$ m fibers, while nodal  $K^+$  channels in 12- $\mu$ m fibers have the same drug specificity as nodal  $K^+$  channels in 16–18- $\mu$ m fibers.

**Discussion.** In prior studies of frog fibers dissociation constants for external 4-AP were 10–20  $\mu$ M and 400  $\mu$ M respectively<sup>4,6</sup>, consistent with the data from nodal  $K^+$  channels in 16–18- $\mu$ m fibers. We have shown that LPC dependent, presumably para-

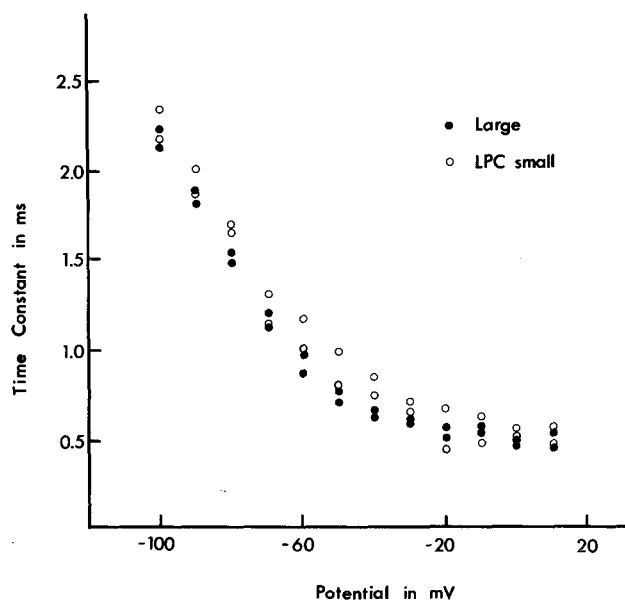


Figure 3. Comparison of the time constants for potassium activation in untreated 16–18- $\mu$ m (solid circles) and LPC-treated 8–10- $\mu$ m fibers (open circles) as a function of membrane potential. There was no significant difference in the temporal behavior of the  $K^+$  conductance in either of the two fibers illustrated.

nodal  $K^+$  channels have a four-fold lower dissociation constant for 4-AP than nodal  $K^+$  channels, while TEA is less effective on paranodal  $K^+$  channels. Others have seen decreased sensitivity of paranodal and internodal  $K^+$  channels to TEA<sup>13,23,36</sup>. For example, 6 mM TEA failed to block outward currents in demyelinated rat fibers and 20 mM only decreased outward currents of paranodally demyelinated rabbit fibers by 30%. Internodal  $K^+$  currents in frog fibers were reduced by 80% by 10 mM TEA, but data on intact nodes predicts a 96% decrease. Reduced sensitivity of internodal channels to TEA has been attributed to limited drug access. Since internodal channels are more sensitive to 4-AP, it is quite likely that differential responses to TEA exist. Several 4-AP derivatives are  $K^+$  channel blockers<sup>5,22,37–39</sup>. The drug 3,4-diaminopyridine (3,4-DAP) has a dissociation constant in squid axons of 6  $\mu$ M<sup>5,39</sup>. In two 16–18- $\mu$ m frog fibers, 5  $\mu$ M 3,4-DAP reduced the  $K^+$  currents by 60–70%, consistent with a 5–6-fold lower dissociation constant. In two LPC-treated 8–10- $\mu$ m fibers, 5  $\mu$ M 3,4-diaminopyridine completely blocked the outward  $K^+$  currents. A similar differential effect on nodal and paranodal  $K^+$  channels seems to hold for 4-AP derivatives. Dose-response curves for 4-AP are not available for paranodal or internodal  $K^+$  channels in mammalian nerve, so direct comparison is not possible. However, 300  $\mu$ M 4-AP doubles the action potential duration in normal nonmyelinated guinea pig vagus<sup>38</sup>, increases it by 30% in remyelinated rabbit nerves, and prolongs it 40–70% in fibers regenerating from a crush injury<sup>18</sup>. While a value for the dissociation constant cannot be obtained from the effects of 4-AP on action potential duration, these data suggest internodal  $K^+$  channels are highly sensitive to 4-AP.

In paranodally demyelinated mammalian fibers  $K^+$  activation resembles that in frog nodes<sup>9</sup>. Using values of the internodal capacitance and resistance obtained from leak and capacity currents in demyelinated frog internodes, Chiu and Ritchie<sup>23</sup> incorporated standard nodal  $K^+$  channel kinetics to calculate  $K^+$  currents similar to those of demyelinated internodes. The actual currents activated faster than predicted, but it is difficult to decide whether such differences are real because of series resistance errors and inadequate spatial control of demyelinated internodes. The results here show that the voltage and time

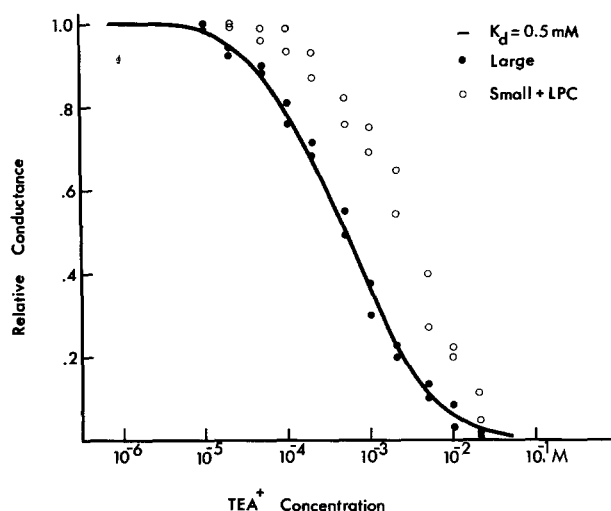


Figure 4. Dose-response curves for tetraethylammonium (TEA) in two different 16–18- $\mu$ m (filled circles) and 8–10- $\mu$ m (open circles) fibers. The ordinate shows the  $K^+$  conductance in the presence of TEA relative to that obtained prior to drug application (the effects of TEA were also readily reversible). The solid line is the expected dissociation curve for a single drug binding site having an effective binding constant of  $0.5 \times 10^{-3}$  M and accurately describes the response of 16–18- $\mu$ m fibers. The behavior of 8–10- $\mu$ m fibers is consistent with a shift of this dissociation curve to the right along the abscissa so that the effective binding constant is increased to  $5 \times 10^{-3}$  M.

dependence of activation of paranodal K<sup>+</sup> channels is the same as nodal channels, even though their pharmacological behavior is quite distinct. Are internodal and paranodal K<sup>+</sup> channels identical? To answer this question one needs to achieve good spatial control by clamping demyelinated internodes in a chamber where the width of the recording pool is 10–20 µm. Even so, such experiments would not be internally controlled and subject to criticism.

Frog nodes have several types of K<sup>+</sup> channels which differ in kinetics and pharmacological sensitivity, and vary in sensory and motor fibers<sup>36</sup>. In this study there were no significant differences in 4-AP and TEA sensitivity between sensory and motor fiber nodal or paranodal channels. Activation of nodal and paranodal K<sup>+</sup> channels appeared similar, but studies of K<sup>+</sup> channel kinetics in myelinated nerve is complicated by K<sup>+</sup> accumulation<sup>36</sup>. Since K<sup>+</sup> tail currents were not measured, it is possible that K<sup>+</sup> channel subpopulation density varies between nodes and paranodes and produces the pharmacological differences observed.

Acknowledgement. Supported by National Multiple Sclerosis Society Grant RG 1911A4 and by National Science Foundation Grant BNS 86-96095.

- 1 Smith, K. J., and Schauf, C. L., *Nature* 293 (1981) 297.
- 2 Pelhate, M., Hue, B., and Chanelet, J., *C. r. Séanc. Soc. Biol.* 166 (1971) 1598.
- 3 Schauf, C. L., Colton, C. A., Colton J. S., and Davis, F. A., *J. Pharmac. exp. Ther.* 197 (1976) 414.
- 4 Ulbricht, W., and Wagner, H. H., *Pflügers Arch.* 367 (1976) 77.
- 5 Kirsch, G., and Narahashi, T., *Biophys. J.* 18 (1978) 507.
- 6 Dubois, J. M., in: *Advances in Biosciences*, vol. 35, pp. 43–51. Ed. P. Lechat. Pergamon Press, New York 1982.
- 7 Quinta-Ferreira, M. E., Rojas, E., and Arispe, N., *J. Membr. Biol.* 66 (1982) 159.
- 8 Horackova, M., Nonner, W., and Stämpfli, R., *Proc. int. Un. physiol. Sci.* 7 (1968) 198.
- 9 Chiu, S. Y., Ritchie, J. M., Rogart, R. B., and Stagg, D., *J. Physiol., Lond.* 292 (1979) 149.
- 10 Brismar, T., *J. Physiol., Lond.* 298 (1980) 171.
- 11 Chiu, S. Y., and Ritchie, J. M., *Nature* 284 (1980) 170.
- 12 Bostock, H., Sears, T. A., and Sherratt, R. M., *J. Physiol., Lond.* 313 (1981) 301.
- 13 Brismar, T., *Acta physiol. scand.* 113 (1981) 167.
- 14 Chiu, S. Y., and Ritchie, J. M., *J. Physiol.* 313 (1981) 415.
- 15 Targ, E. F., and Kocis, J. D., *Brain Res.* 328 (1985) 358.
- 16 Waxman, S. G., Kocis, J. D., and Eng, D. L., *Muscle Nerve* 8 (1985) 85.
- 17 Kocis, J. D., Bowe, C. M., and Waxman, S. G., *Neurology* 36 (1986) 117.
- 18 Ritchie, J. M., *Proc. R. Soc., Lond. B* 215 (1982) 273.
- 19 Kocis, J. D., and Waxman, S. G., *Nature* 304 (1983) 640.
- 20 Bowe, C. M., Kocis, J. D., and Waxman, S. G., *Proc. R. Soc., Lond. B* 224 (1985) 355.
- 21 Kocis, J. D., in: *Ion Channels in Neural Membranes*, pp. 123–144. Eds Ritchie, Keynes and Bolis. Alan Liss, Publ., New York 1986.
- 22 Kiloh, N., Harvey, A. L., and Glover, W. E., *Eur. J. Pharmac.* 70 (1981) 53.
- 23 Chiu, S. Y., and Ritchie, J. M., *J. Physiol.* 322 (1982) 485.
- 24 Pencek, T. L., Schauf, C. L., Low, P. S., Eisenberg, B. R., and Davis, F. A., *Neurology* 30 (1980) 593.
- 25 Jones, R. E., Heron, J. R., Foster, D. H., Snelgar, R. S., and Mason, R. J., *J. neurol. Sci.* 60 (1983) 353.
- 26 Stefoski, D., Davis, F. A., Faut, M., and Schauf, C. L., *Ann. Neurol.* (1986) in press.
- 27 Dubois, J. M., *Proc. Biophys. molec. Biol.* 42 (1983) 1.
- 28 Targ, E. F., and Kocis, J. D., *Brain Res.* 363 (1986) 1.
- 29 Dodge, F. A., and Frankenhauser, B., *J. Physiol.* 143 (1968) 76.
- 30 Pencek, T. L., Schauf, C. L., and Davis, F. A., *J. Pharmac. exp. Ther.* 204 (1978) 400.
- 31 Schmidt, H., and Stampfli, R., *Helv. physiol. pharmac. Acta* 22 (1964) C143.
- 32 Hille, B., *Biophysics and Physiology of Excitable Membranes*, pp. 230–246. Ed. W. J. Adelman. Van Nostrand Reinhold, New York 1971.
- 33 Sigworth, F. J., Ph. D. thesis. Yale University, New Haven 1979.
- 34 Bergman, C., *Pflügers Arch.* 317 (1970) 287.
- 35 Brismar, T., *Pflügers Arch.* 393 (1982) 348.
- 36 Dubois, J. M., *J. Physiol.* 318 (1981) 297.
- 37 Molgo, J., Lundh, H., and Thesleff, S., *Eur. J. Pharmac.* 61 (1980) 25.
- 38 Den Hertog, A., Pielkenrood, J., Biessels, P., and Agoston, S., *Eur. J. Pharmac.* 94 (1983) 353.
- 39 Kirsch, G., and Narahashi, T., *J. Pharmac. exp. Ther.* 226 (1983) 174.

0014-4754/87/040405-04\$1.50 + 0.20/0  
© Birkhäuser Verlag Basel, 1987

## Regional brain [Met]-enkephalin in alcohol-preferring and non-alcohol-preferring inbred strains of mice

K. Blum, A. H. Briggs, J. E. Wallace\*, C. W. Hall\*\* and M. A. Trachtenberg\*\*\*

*Departments of Pharmacology and Pathology, \*University of Texas Health Science Center, and \*\*Southwest Research Institute, San Antonio (Texas 78284, USA), and \*\*\*Matrix Technologies, Inc., Houston (Texas 77058, USA), 19 June 1986*

**Summary.** Scrutiny of the data from these studies reveals that the C58/J alcohol-preferring mice have significantly lower baseline methionine-enkephalin levels in both the corpus striatum and hypothalamus compared to C3H/CHRG/2 non-alcohol-preferring mice. In other brain regions in these two strains, specifically, pituitary, amygdala, midbrain, and hippocampus, analysis of methionine-enkephalin levels did not show any significant differences. This suggests that the hypothalamus may indeed be a specific locus involved in the regulation of alcohol intake, via the molecular interaction between neuroamines, opioid peptides, as they are influenced by genetics and environment.

**Key words.** Opioid peptides; methionine-enkephalin; alcohol-avoiding mice; alcohol-preferring mice; hypothalamus; corpus striatum.

Numerous studies have attempted to establish a relationship between brain neurotransmitters and neuropeptides and alcohol-drinking behavior. Blum et al.<sup>1</sup> have previously shown that there is correlation between whole brain methionine-enkephalin ([Met]-enk) and amounts of alcohol consumed. Using a 14-day preference test, an estimated correlation of 0.909 was found between mouse whole brain [Met]-enk levels and alcohol consumption in alcohol-preferring (C57BL/6J, C58/6J) and alcohol avoiding strains (DBA/2J and C3H/CHRG/2). In that study,

C57BL/6J and C58/6J mice, which drank more alcohol than the DBA/2J and C3H strains, exhibited significantly less brain [Met]-enk. In later studies, Blum et al.<sup>2</sup> discovered that a sub-strain of the C57BL group, specifically C57BL/6N, supplied by the Simonsen laboratories, reverted to more normal alcohol consumption levels. Examination of [Met]-enk brain levels in this substrain revealed significantly higher levels as compared to C57B/6J mice<sup>3</sup>. C57BL/6J and DBA/2J exhibited individual differences in alcohol-drinking behavior when tested in a 1-day